Hadronic light-by-light contribution to the magnetic moment of the muon from lattice QCD: status of Mainz calculations

Harvey Meyer
Johannes Gutenberg University Mainz

Seventh plenary workshop of the muon g-2 Theory Initiative, KEK, Tsukuba, 12 September 2024

PRiSMA+
Cluster of Excellence

Hadrons CRC 1660 Nuclei

erc
European Research Council
Established by the European Commission

Source of dominant uncertainties in SM

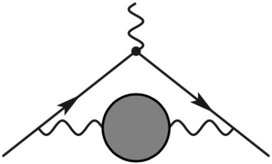

Hadronic vacuum polarisation

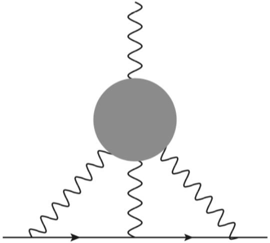

Hadronic light-by-light scattering

HVP: O(α^2), about $700 \cdot 10^{-10}$

WP20 precision: 0.6%

Desirable precision: 0.2%

HLbL: O(α^3), about $10 \cdot 10^{-10}$

WP20 precision: 20%.

Desirable precision: 10%.

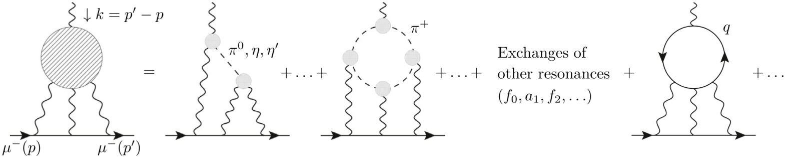

Selected literature

1. Hayakawa, Blum, Izubuchi, Yamada hep-lat/0509016 (LAT'05, Dublin); 1407.2923.
2. Blum et al. 1510.0710; 1610.0460; **1911.0812** (results with QED in finite volume);
3. Blum et al. 1705.0106 (QED in infinite volume, tested on free quark loop computed on the lattice); Blum et al. **2304.04423** (results);
4. Mainz group conference proceedings: 1510.08384, 1609.08454, 1711.02466, 1801.04238, 1811.08320, 1911.05573.
5. Mainz group: 2006.16224 (at $SU(3)_f$ symmetric point); **2104.02632** (extrapolating to physical quark masses); **2204.08844** (charm contribution).
6. Mainz QED kernel: 2210.12263. Available at `https://github.com/RJHudspith/KQED`
7. 2311.10628 & Lattice'24 Zimmermann, Gérardin; Lattice'24 Kanwar, Petschlies, Kalntis, Romiti, Wenger (ETMC).

Coordinate-space approach to a_μ^{HLbL}

QED kernel $\mathcal{L}_{[\rho,\sigma];\mu\nu\lambda}(p,x,y)$

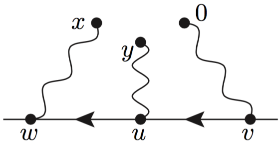

$\Rightarrow$

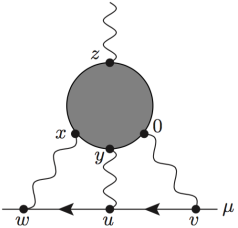

$$a_\mu^{\mathrm{HLbL}} = \frac{me^6}{3}\int d^4y \Big[\int d^4x \underbrace{\mathcal{L}_{[\rho,\sigma];\mu\nu\lambda}(p,x,y)}_{\mathrm{QED}} \; \underbrace{i\widehat{\Pi}_{\rho;\mu\nu\lambda\sigma}(x,y)}_{=\mathrm{QCD\ blob}}\Big].$$

$$i\widehat{\Pi}_{\rho;\mu\nu\lambda\sigma}(x,y) = -\int d^4z \; z_\rho \Big\langle j_\mu(x)\, j_\nu(y)\, j_\sigma(z)\, j_\lambda(0)\Big\rangle.$$

- on-shell muon momentum realized as $p = (iE_{\boldsymbol{p}}, \boldsymbol{p})$. Simplest choice $p = (im, \boldsymbol{0})$.
- $\mathcal{L}_{[\rho,\sigma];\mu\nu\lambda}(p,x,y)$ computed in the continuum & infinite-volume
- no power-law finite-volume effects.

Coordinate-space approach to a_μ^{HLbL}: version used by Mainz

QED kernel $\bar{\mathcal{L}}_{[\rho,\sigma];\mu\nu\lambda}(x,y)$

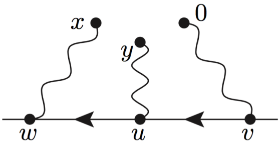

$\Rightarrow$

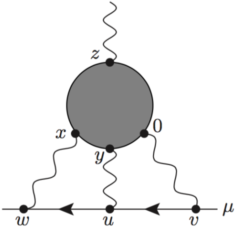

$$a_\mu^{\mathrm{HLbL}} = \frac{me^6}{3} \underbrace{\int d^4y}_{=2\pi^2|y|^3 d|y|} \Big[\int d^4x\, \underbrace{\bar{\mathcal{L}}_{[\rho,\sigma];\mu\nu\lambda}(x,y)}_{\mathrm{QED}}\; \underbrace{i\widehat{\Pi}_{\rho;\mu\nu\lambda\sigma}(x,y)}_{=\mathrm{QCD\ blob}}\Big].$$

- only a 1d integral to sample the integrand in $|y|$ thanks to analytic average over muon momentum.

[Asmussen, Gérardin, Green, HM, Nyffeler 1510.08384.]

Notation: connection between RBC/UKQCD and Mainz

$$\mathfrak{G}^{\rm RBC}_{\mu\nu\lambda}(x,y,z) = (-i)\frac{1+\gamma_0}{2} K^{\rm Mainz}_{\mu\nu\lambda}(p=(im,\mathbf{0}),x-z,y-z)\frac{1+\gamma_0}{2}$$

$$\frac{i}{4}\,{\rm Tr}\{[\gamma_\rho,\gamma_\sigma]\mathfrak{G}^{\rm RBC}_{\mu\nu\lambda}(x,y,0)\} = \mathcal{L}^{\rm Mainz}_{[\rho,\sigma];\mu\nu\lambda}(p=(im,\mathbf{0}),x,y).$$

$$6i\int d^4x_{\rm op}\;(x_{\rm op}-x_{\rm ref})_j\;\mathcal{H}^{\rm RBC}_{k,\rho,\sigma,\lambda}(x_{\rm op},x,y,z) = \widehat{\Pi}^{\rm Mainz}_{j;\rho\sigma\lambda k}(x-z,y-z).$$

This should make it possible to describe the various lattice calculations in a single notation in the White Paper.

RBC/UKQCD 2304.04423 vs. Mainz 2210.12263

Isospin decomposition vs. quark-level Wick contractions

$$V^{\text{e.m.}} = V^3 + V^8, \quad V^3 = \tfrac{1}{2}(\bar{u}\gamma u - \bar{d}\gamma d), \quad V^8 = \tfrac{1}{6}(\bar{u}\gamma u + \bar{d}\gamma d - 2\bar{s}\gamma s)$$

$$\begin{aligned}
\Pi^{\text{HLbL}} &= \langle V^{\text{e.m.}}_{X_1} V^{\text{e.m.}}_{X_2} V^{\text{e.m.}}_{X_3} V^{\text{e.m.}}_{X_4} \rangle, \\
\Pi^{\{3333\}} &= \langle V^3_{X_1} V^3_{X_2} V^3_{X_3} V^3_{X_4} \rangle, \\
\Pi^{\{8888\}} &= \langle V^3_{X_1} V^3_{X_2} V^3_{X_3} V^3_{X_4} \rangle \\
\Pi^{\{3838\}} &= \frac{1}{2!2!} \sum_{\mathcal{P} \in \mathcal{S}_4} \langle V^8_{X_{\mathcal{P}(1)}} V^3_{X_{\mathcal{P}(2)}} V^8_{X_{\mathcal{P}(3)}} V^3_{X_{\mathcal{P}(4)}} \rangle,
\end{aligned}$$

$$\Pi^{\text{HLbL}} = \Pi^{\{3333\}} + \Pi^{\{8888\}} + \Pi^{\{3838\}}.$$

Wick-contraction topologies in HLbL amplitude $\langle 0 | T\{ j^\mu_x j^\nu_y j^\lambda_z j^\sigma_0 \} | 0 \rangle$

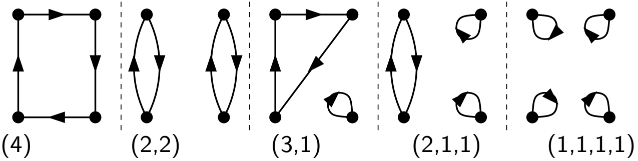

Charge factors of the quark-level diagrams

In the (u, d) quark sector, the five diagram classes appear with the following the charge factors:

	$\Pi^{(4)}$	$\Pi^{(2,2)}$	$\Pi^{(3,1)}$	$\Pi^{(2,1,1)}$	$\Pi^{(1,1,1,1)}$
$\Pi^{\{3333\}}$	$\frac{1}{8}$	$\frac{1}{4}$	0	0	0
$\Pi^{\{8888\}}$	$\frac{1}{648}$	$\frac{1}{324}$	$\frac{1}{324}$	$\frac{1}{162}$	$\frac{1}{81}$
$\Pi^{\{3838\}}$	$\frac{1}{12}$	$\frac{1}{18}$	$\frac{1}{12}$	$\frac{1}{18}$	0
Total: Π^{HLbL}	$\frac{17}{81}$	$\frac{25}{81}$	$\frac{7}{81}$	$\frac{5}{81}$	$\frac{1}{81}$

e.g. the set of fully connected diagrams $\Pi^{(4)}$ appears with charge factor $((\frac{2}{3})^4 + (-\frac{1}{3})^4) = \frac{17}{81}$ in the HLbL amplitude.

Exchange of an isovector meson (π^0, ...)

The π^0 exchange (or of any other isovector meson) appears only in Π^{3388}.
The fact that it vanishes in Π^{3333} implies the ratio

$$\left[\frac{25}{81}\Pi^{(2,2;\pi^0)}\right] = -\frac{25}{34}\left[\frac{17}{81}\Pi^{(4,\pi^0)}\right]. \quad (1)$$

Neglecting the diagrams containing three quark loops or more, the contribution $\Pi^{\mathrm{HLbL};\pi^0}$ to HLbL amplitude is partitioned according to

$$\left[\frac{17}{81}\Pi^{(4;\pi^0)}\right] = \frac{34}{9}\,\Pi^{\mathrm{HLbL};\pi^0},$$
$$\left[\frac{25}{81}\Pi^{(2,2;\pi^0)}\right] = -\frac{25}{9}\,\Pi^{\mathrm{HLbL};\pi^0}.$$

First derived by J. Bijnens, 1608.01454.

Similarly, for an isoscalar meson exchange (say, (f_2)): if you assume that the meson couples equally to a pair (V_μ^3, V_ν^3) as to the pair $(3V_\mu^8, 3V_\nu^8)$, then you find that its entire contribution to Π^{HLbL} is contained in $\left[\frac{25}{81}\Pi^{(2,2;\pi^0)}\right]$.

See 1712.00421.

The charged pion loop

At leading order in ChPT, the charged pion loop appears only in $\Pi^{\{3333\}}$.

From this observation, neglecting the diagrams containing three quark loops or more, one finds that the charged pion loop contribution $\Pi^{\mathrm{HLbL};\pi\pi}$ to HLbL amplitude is partitioned across $\Pi^{(4)}$, $\Pi^{(2,2)}$ and $\Pi^{(3,1)}$ diagrams according to

$$\begin{aligned}\left[\frac{17}{81}\Pi^{(4;\pi\pi)}\right] &= \frac{34}{81}\,\Pi^{\mathrm{HLbL};\pi\pi},\\ \left[\frac{25}{81}\Pi^{(2,2;\pi\pi)}\right] &= \frac{75}{81}\,\Pi^{\mathrm{HLbL};\pi\pi},\\ \left[\frac{7}{81}\Pi^{(3,1;\pi\pi)}\right] &= -\frac{28}{81}\,\Pi^{\mathrm{HLbL};\pi\pi}.\end{aligned}$$

See 2104.02632 apdx A for a partially quenched ChPT derivation.

Integrand of connected contribution at $m_\pi = 200$ MeV

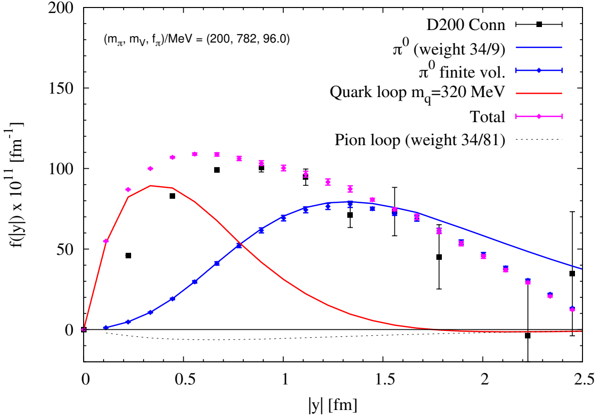

- Semi-quantitative description of the integrand;
- Cutoff effects at short distances.

2104.02632

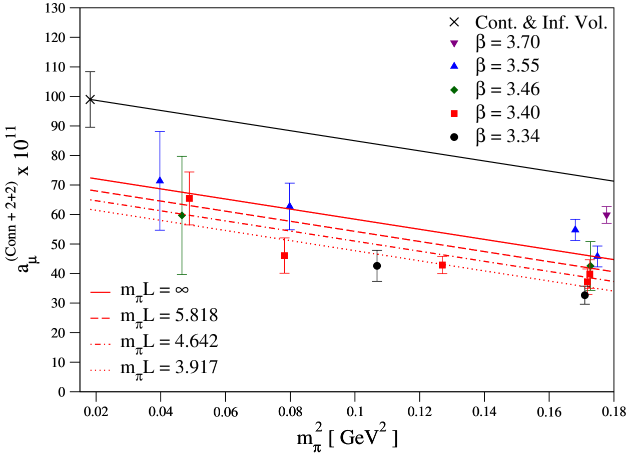

Chiral & continuum limit linear in m_π^2 and a^2 for the $(Q_u^4 + Q_d^4)\Pi^{(4)} + (Q_u^2 + Q_d^2)^2\Pi^{(2,2)}$ contribution.

2104.02632

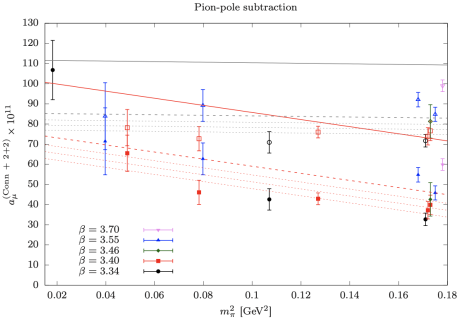

Figure 8: Red lines: original tail-reconstructed data. Black lines: with π^0-exchange computed on each ensemble individually subtracted and the continuum value added back at the physical pion mass. The dotted lines and dashed lines correspond to finite $m_\pi L$ (see Fig. 3) and infinite $m_\pi L$ at fixed $\beta = 3.4$ respectively and the plain lines are the results in the continuum and infinite-volume limit. The data point at the top left corner corresponds to our quoted final estimate for a_μ^{hlbl}.

E.-H. Chao, LAT21.

Overview table

Contribution	Value$\times 10^{11}$
Light-quark fully-connected and $(2+2)$	107.4(11.3)(9.2)(6.0)
Strange-quark fully-connected and $(2+2)$	$-0.6(2.0)$
$(3+1)$	0.0(0.6)
$(2+1+1)$	0.0(0.3)
$(1+1+1+1)$	0.0(0.1)
Total	106.8(15.9)

- error dominated by the statistical error and the continuum limit.
- all subleading contributions have been tightly constrained and shown to be negligible.

[Chao et al, 2104.02632]

Result for charm: $a_\mu(\text{charm}) = (2.8 \pm 0.5) \times 10^{-11}$.

Compilation of $a_\mu^{\rm HLbL}$ determinations

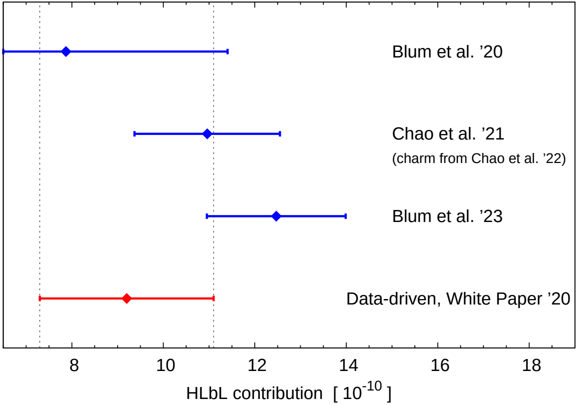

Good consistency of different determinations.
Lattice'24: $a_\mu^{\rm HLbL} = 12.6(1.2)(3) \cdot 10^{-10}$ (Ch. Zimmermann, BMW).

Results from the Bern dispersive framework and from three independent lattice QCD calculations since 2021 are in agreement with comparable uncertainties.

How best to combine the lattice results for a_μ^{HLbL}

The statistical errors of different calculations are uncorrelated (except e.g. for the charm contribution if it is taken from the Mainz calculation).

Dominant systematic errors:

- Continuum limit needs to be consolidated; how strongly does the slope in a^2 depend on the quark mass?
- Treatment of long-distances is based on the same idea that the π^0 exchange dominates.
- Fit ansätze for the m_π dependence related to the same physics.

Thus it is not clear that one can do better than treating the systematic error as being 100% correlated across different calculations.

Backup slides

The charm contribution at the SU(3)$_\mathrm{f}$ point

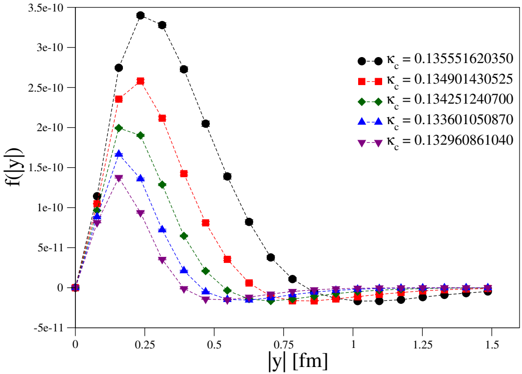

Integrand for the connected charm contribution (J500, $a = 0.039\,\mathrm{fm}$)

- direct calculation at physical charm mass difficult due to lattice artefacts
- $\rightsquigarrow$ perform a combined extrapolation in $1/m_c^2$ and the lattice spacing.

Chao, Hudspith, Gérardin, Green, HM arXiv:2204.08844

Extrapolation in charm mass and lattice spacing

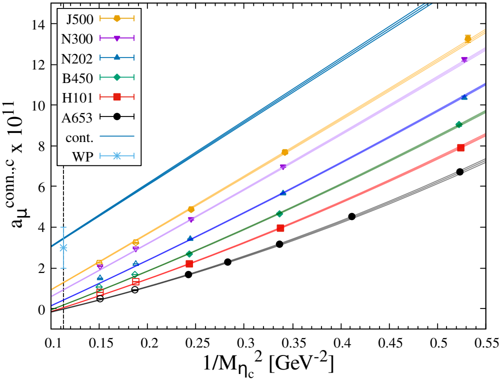

This particular fit:

$$a_\mu(a, m_{\eta_c}) = Aa + \frac{B + Ca^2}{m_{\eta_c}^2} + Da^2 + E\frac{a^2}{m_{\eta_c}^4}$$

Final result (average of several fits): $a_\mu(\mathrm{charm}) = (2.8 \pm 0.5) \times 10^{-11}$.

Truncated integral for a_μ^{HLbL}

Connected

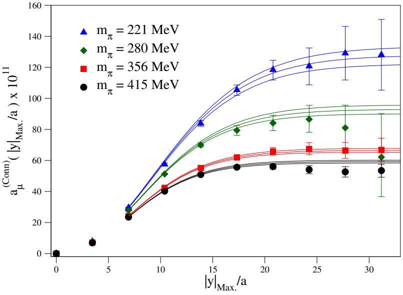

(2+2) Disconnected

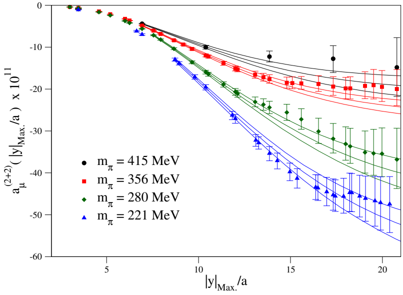

- Extend reach of the signal by two-param. fit $f(y) = A|y|^3 \exp(-M|y|)$;
- provides an excellent description of the π^0 exchange contribution in infinite volume.
- We see a clear increase of the magnitude of both connected and disconnected contributions.

Chiral, continuum, volume extrapolation

Connected contribution

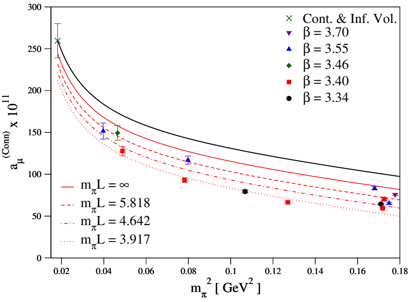

disconnected contribution

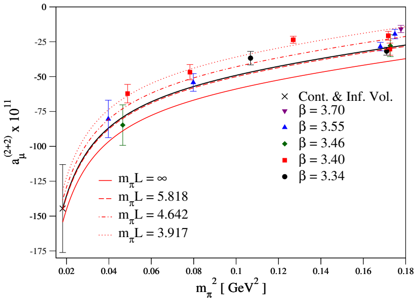

Total light-quark contribution:

- vol. dependence: $\propto \exp(-m_\pi L/2)$
- pion-mass dependence fairly mild (!)

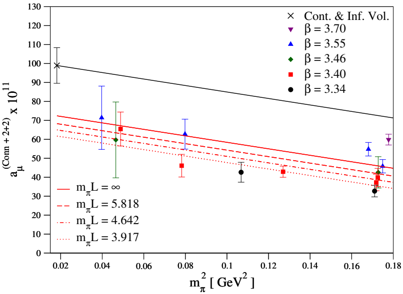

$a_\mu^{\rm HLbL}$ at $m_\pi = m_K \simeq 415$ MeV: continuum limit

[Chao, Gérardin, Green, Hudspith, HM 2006.16224 (EPJC)]

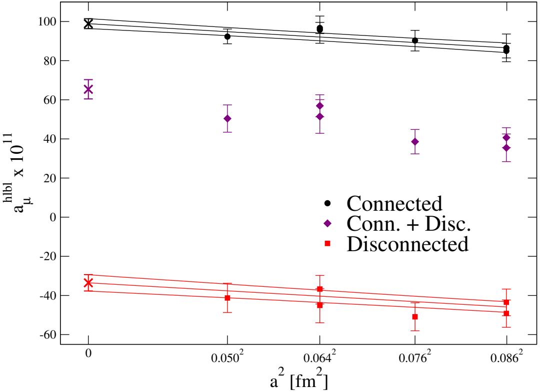

$$a_\mu^{\rm hlbl, SU(3)_f} = (65.4 \pm 4.9 \pm 6.6) \times 10^{-11}.$$

Rearrangement of integrals: 'method 2'

For the fully-connected calculation we use the following master equation for the integrand:

$$f^{(\text{Conn.})}(|y|) = -\sum_{j\in u,d,s} \hat{Z}_{\mathrm{V}}^4 Q_j^4 \frac{m_\mu e^6}{3} 2\pi^2 |y|^3 \times$$

$$\int_x \left(\mathcal{L}'_{[\rho,\sigma]\mu\nu\lambda}(x,y) \int_z z_\rho \widetilde{\Pi}^{(1),j}_{\mu\nu\sigma\lambda}(x,y,z) + \bar{\mathcal{L}}^{(\Lambda)}_{[\rho,\sigma];\lambda\nu\mu}(x,x-y) x_\rho \int_z \widetilde{\Pi}^{(1),j}_{\mu\nu\sigma\lambda}(x,y,z) \right),$$

with hadronic contribution

$$\widetilde{\Pi}^{(1),j}_{\mu\nu\sigma\lambda}(x,y,z) = -2\text{Re}\left\langle \mathrm{Tr}\left[S^j(0,x)\gamma_\mu S^j(x,y)\gamma_\nu S^j(y,z)\gamma_\sigma S^j(z,0)\gamma_\lambda \right] \right\rangle_U .$$

- $S^j(x,y)$ is the flavour j-quark propagator from source y to sink x;
- Q_j is the charge factor ($Q_u = \frac{2}{3}$, $Q_d = -\frac{1}{3}$, $Q_s = -\frac{1}{3}$);
- $\langle\cdot\rangle_U$ denotes the ensemble average.

$$\mathcal{L}'_{[\rho,\sigma];\mu\nu\lambda}(x,y) = \bar{\mathcal{L}}^{(\Lambda)}_{[\rho,\sigma];\mu\nu\lambda}(x,y) + \bar{\mathcal{L}}^{(\Lambda)}_{[\rho,\sigma];\nu\mu\lambda}(y,x) - \bar{\mathcal{L}}^{(\Lambda)}_{[\rho,\sigma];\lambda\nu\mu}(x,x-y).$$

HLbL & the projection formula

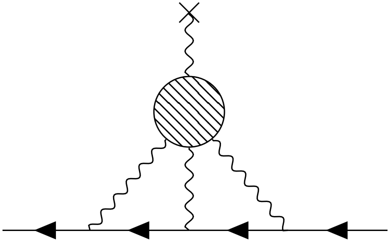

$$a_\mu^{\rm HLbL} = F_2(0) = \frac{-i}{48m}\,{\rm Tr}\{[\gamma_\rho,\gamma_\sigma](-i\not{p}+m)\Gamma_{\rho\sigma}(p,p)(-i\not{p}+m)\}\Big|_{p^2=-m^2}\;.$$

The HLbL contribution to the vertex function reads

$$\Gamma_{\rho\sigma}(p',p) \;=\; -e^6\int_{q_1,q_2}\frac{1}{q_1^2q_2^2(q_1+q_2-k)^2}\,\frac{1}{(p'-q_1)^2+m^2}\,\frac{1}{(p'-q_1-q_2)^2+m^2}$$
$$\times\Big(\gamma_\mu(i\not{p}'-i\not{q}_1-m)\gamma_\nu(i\not{p}'-i\not{q}_1-i\not{q}_2-m)\gamma_\lambda\Big)$$
$$\times\frac{\partial}{\partial k_\rho}\Pi_{\mu\nu\lambda\sigma}(q_1,q_2,k-q_1-q_2),$$

$$\Pi_{\mu\nu\lambda\rho}(q_1,q_2,q_3) = \int_{x,y,z} e^{-i(q_1\cdot x+q_2\cdot y+q_3\cdot z)}\Big\langle j_\mu(x)j_\nu(y)j_\lambda(z)j_\rho(0)\Big\rangle_{\rm QCD}.$$

Transition to a Euclidean coordinate-space representation

- Interchange the integrals over momenta and positions:

$$\Gamma_{\rho\sigma}(p,p) \;=\; -e^6 \int_{x,y} K_{\mu\nu\lambda}(p,x,y)\, \widehat{\Pi}_{\rho;\mu\nu\lambda\sigma}(x,y),$$

with the QED kernel

$$K_{\mu\nu\lambda}(p,x,y) \quad = \quad \gamma_\mu(i\not{p} + \not{\partial}^{(x)} - m)\gamma_\nu(i\not{p} + \not{\partial}^{(x)} + \not{\partial}^{(y)} - m)\gamma_\lambda\, \mathcal{I}(p,x,y)_{\text{IR reg.}}\,,$$

$$\mathcal{I}(p,x,y)_{\text{IR reg.}} \quad = \quad \int_{q,k} \frac{1}{q^2\,k^2\,(q+k)^2}\,\frac{1}{(p-q)^2+m^2}\,\frac{1}{(p-q-k)^2+m^2}\; e^{-i(q\cdot x+k\cdot y)}\,.$$

and

$$\widehat{\Pi}_{\rho;\mu\nu\lambda\sigma}(x,y) \;=\; \int_z iz_\rho\, \Big\langle j_\mu(x) j_\nu(y) j_\sigma(z) j_\lambda(0)\Big\rangle_{\text{QCD}}$$

An infrared divergence in the scalar function $\mathcal{I}$ cancels out upon evaluating the Dirac trace and the derivatives.

Simplifying the trace...

$$a_\mu^{\rm HLbL} = \frac{me^6}{3} \int_{x,y} \mathcal{L}_{[\rho,\sigma];\mu\nu\lambda}(p,x,y)\, i\widehat{\Pi}_{\rho;\mu\nu\lambda\sigma}(x,y),$$

with the QED kernel given by

$$\mathcal{L}_{[\rho,\sigma];\mu\nu\lambda}(p,x,y) = \frac{1}{16m^2} {\rm Tr}\Big\{(-i\not{p}+m)[\gamma_\rho,\gamma_\sigma](-i\not{p}+m)K_{\mu\nu\lambda}(p,x,y)\Big\}$$

But what about p, the muon momentum, in Euclidean space?

On-shell muon: $p = (iE_{\boldsymbol{p}}, \boldsymbol{p})$.

Simplest choice: $p = (im, \mathbf{0})$, or more generally $p = im\hat{\epsilon}$, ϵ a unit vector.

$N_{\mathrm{f}} = 2+1$ CLS ensembles used towards physical quark masses

	(4)	(22)	(31)	(211)	(1111)	β	$(a \text{ GeV})^2$	$(\frac{m_\pi}{\text{GeV}})^2$	$(\frac{m_K}{\text{GeV}})^2$	$m_\pi L$	$\hat{Z}_{\mathrm{V}}$
A653	l, s	l, s	0	0	0	3.34	**0.2532**	**0.171**	**0.171**	**5.31**	**0.70351**
A654	l, s	l, s	l				**0.2532**	**0.107**	**0.204**	**4.03**	**0.69789**
U103	l, s	l, s	0	0	0	3.40	0.1915	0.172	0.172	4.35	0.71562
H101	l, s	l, s	0	0	0		0.1915	0.173	0.173	5.82	0.71562
U102	l	l	l				0.1915	0.127	**0.194**	3.74	0.71226
H105	l, s	l, s	l, s				0.1915	0.0782	0.213	3.92	0.70908
C101	l, s	l, s	l, s	l	l, s		0.1915	0.0488	0.237	4.64	0.70717
B450	l, s	l, s	0	0	0	3.46	0.1497	0.173	0.173	5.15	0.72647
D450	l	l	l				0.1497	**0.0465**	0.226	**5.38**	**0.71921**
H200	l, s	l, s	0	0	0	3.55	0.1061	0.175	0.175	4.36	0.74028
N202	l, s	l, s	0	0	0		0.1061	0.168	0.168	6.41	0.74028
N203			l	l			0.1061	0.120	0.194	5.40	0.73792
N200	l	l	l				0.1061	0.0798	0.214	4.42	0.73614
D200	l	l	l				0.1061	0.0397	0.230	4.15	0.73429
N300	l, s	l, s	0	0	0	3.70	0.06372	0.178	0.178	5.11	0.75909

En-Hung Chao, Renwick Hudspith, Antoine Gérardin, Jeremy Green, HM, Konstantin Ottnad
2104.02632 (EPJC)

Tests of the framework and adjustments to the kernel

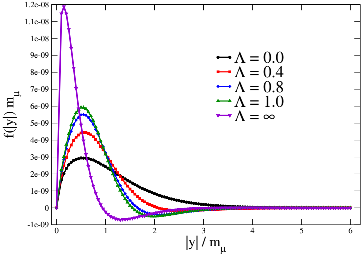

Integrands (Lepton loop, method 2)

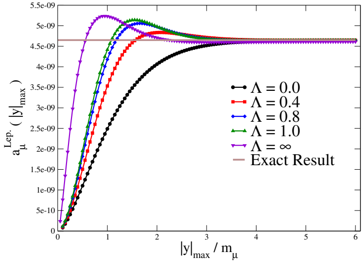

Correspondings integrals

- The QED kernel $\bar{\mathcal{L}}_{[\rho,\sigma];\mu\nu\lambda}(x,y)$ is parametrized by six 'weight' functions of the variables $(x^2, x\cdot y, y^2)$.
-
$$\begin{aligned}\bar{\mathcal{L}}^{(\Lambda)}_{[\rho,\sigma];\mu\nu\lambda}(x,y) =& \bar{\mathcal{L}}_{[\rho,\sigma];\mu\nu\lambda}(x,y) - \partial^{(x)}_\mu (x_\alpha e^{-\Lambda m_\mu^2 x^2/2}) \bar{\mathcal{L}}_{[\rho,\sigma];\alpha\nu\lambda}(0,y) \\ & - \partial^{(y)}_\nu (y_\alpha e^{-\Lambda m_\mu^2 y^2/2}) \bar{\mathcal{L}}_{[\rho,\sigma];\mu\alpha\lambda}(x,0),\end{aligned}$$
- Using this kernel, we have reproduced (at the 1% level) known results for a range of masses for:
  1. the lepton loop (spinor QED, shown in the two plots);
  2. the charged pion loop (scalar QED);
  3. the π^0 exchange with a VMD-parametrized transition form factor.

Averaging over the direction of the muon momentum

We arrive at

$$a_\mu^{\rm HLbL} = \frac{me^6}{3}\int_{x,y} \bar{\mathcal{L}}_{[\rho,\sigma];\mu\nu\lambda}(x,y)\; i\widehat{\Pi}_{\rho;\mu\nu\lambda\sigma}(x,y),$$

with

$$\begin{aligned}\bar{\mathcal{L}}_{[\rho,\sigma];\mu\nu\lambda}(x,y) \;=\;& \mathcal{G}^{\rm I}_{\delta[\rho,\sigma]\mu\alpha\nu\beta\lambda}\,\langle\hat\epsilon_\delta\partial^{(x)}_\alpha(\partial^{(x)}_\beta+\partial^{(y)}_\beta)\mathcal{I}\rangle_{\hat\epsilon}\\ &+m\,\mathcal{G}^{\rm II}_{\delta[\rho,\sigma]\mu\alpha\nu\beta\lambda}\langle\hat\epsilon_\delta\hat\epsilon_\beta\;\partial^{(x)}_\alpha\mathcal{I}\rangle_{\hat\epsilon}\\ &+m\,\mathcal{G}^{\rm III}_{\delta[\rho,\sigma]\mu\alpha\nu\beta\lambda}\,\langle\hat\epsilon_\alpha\hat\epsilon_\delta(\partial^{(x)}_\beta+\partial^{(y)}_\beta)\mathcal{I}\rangle_{\hat\epsilon},\end{aligned}$$

where we have defined

$$\begin{aligned}\mathcal{G}^{\rm I}_{\delta[\rho,\sigma]\mu\alpha\nu\beta\lambda} &\equiv \frac{1}{8}{\rm Tr}\Big\{\Big(\gamma_\delta[\gamma_\rho,\gamma_\sigma]+2(\delta_{\delta\sigma}\gamma_\rho-\delta_{\delta\rho}\gamma_\sigma)\Big)\gamma_\mu\gamma_\alpha\gamma_\nu\gamma_\beta\gamma_\lambda\Big\},\\ \mathcal{G}^{\rm II}_{\delta[\rho,\sigma]\mu\alpha\nu\beta\lambda} &\equiv -\frac{1}{4}{\rm Tr}\Big\{\Big(\gamma_\delta[\gamma_\rho,\gamma_\sigma]+2(\delta_{\delta\sigma}\gamma_\rho-\delta_{\delta\rho}\gamma_\sigma)\Big)\gamma_\mu\gamma_\alpha\gamma_\nu\Big\}\;\delta_{\beta\lambda},\\ \mathcal{G}^{\rm III}_{\delta[\rho,\sigma]\mu\alpha\nu\beta\lambda} &\equiv -\frac{1}{4}{\rm Tr}\Big\{\Big(\gamma_\delta[\gamma_\rho,\gamma_\sigma]+2(\delta_{\delta\sigma}\gamma_\rho-\delta_{\delta\rho}\gamma_\sigma)\Big)\gamma_\mu(\delta_{\alpha\lambda}\gamma_\nu\gamma_\beta-\delta_{\alpha\beta}\gamma_\nu\gamma_\lambda+\delta_{\alpha\nu}\gamma_\beta\gamma_\lambda)\Big\}.\end{aligned}$$

The tensors $\mathcal{G}^{\rm A}_{\delta[\rho,\sigma]\mu\alpha\nu\beta\lambda}$ are sums of products of Kronecker deltas.

The scalar function $\mathcal{I}$

Recall:

$$\mathcal{I}(p,x,y)_{\rm IR\ reg.} \quad = \quad \int_{q,k} \frac{1}{q^2\, k^2\, (q+k)^2}\, \frac{1}{(p-q)^2+m^2}\, \frac{1}{(p-q-k)^2+m^2}\; e^{-i(q\cdot x+k\cdot y)}\,.$$

In terms of position-space propagators, we can write it as

$$\begin{aligned} \mathcal{I}(p=im\hat\epsilon,x,y) &= \int_u G_0(y-u)\, J(\hat\epsilon,u)\, J(\hat\epsilon,x-u)\,, \\ J(\hat\epsilon,u) &= \int_{\tilde u} G_0(u-\tilde u) e^{m\hat\epsilon\cdot\tilde u}\, G_m(\tilde u)\,. \end{aligned}$$

The function $J(\hat\epsilon,u)$ represents the amplitude for a scalar particle to start from the origin, emit a photon that reaches spacetime-point u, and emerge on-shell.

Propagators in Euclidean:

$$\begin{aligned} G_0(x-y) &= \int_k \frac{e^{ik\cdot(x-y)}}{k^2} = \frac{1}{4\pi^2(x-y)^2}\,, \\ G_m(x-y) &= \int_k \frac{e^{ik\cdot(x-y)}}{k^2+m^2} = \frac{m}{4\pi^2|x-y|} K_1(m|x-y|)\,, \end{aligned}$$

The function $J(\hat\epsilon, u)$

Its expansion in $\lambda = 1$ Gegenbauer polynomials
(analogue for $d = 4$ of Legendre polynomials for $d = 3$):

$$J(\hat\epsilon, u) = \frac{1}{8\pi^2 m|u|}\int_0^{m|u|} dt\, e^{t\hat\epsilon\cdot\hat u}\, K_0(t) = \sum_{n=0}^{\infty} z_n(u^2)\, C_n(\hat\epsilon\cdot\hat u),$$

$$z_n(u^2) = \frac{1}{4\pi^2}\Big[I_{n+2}(m|u|)\frac{K_0(m|u|)}{n+1} + I_{n+1}(m|u|)\Big(\frac{K_1(m|u|)}{n+1} + \frac{K_0(m|u|)}{m|u|}\Big)\Big],$$

The average of the scalar, vector, tensor components of $J(\hat\epsilon, u)\, J(\hat\epsilon, x-u)$ over $\hat\epsilon$ is done analytically *before* the u integral.

The final u integral is reduced to one angular, one radial integral, which were done numerically.

Integrand at $m_\pi = m_K \simeq 415\,$MeV

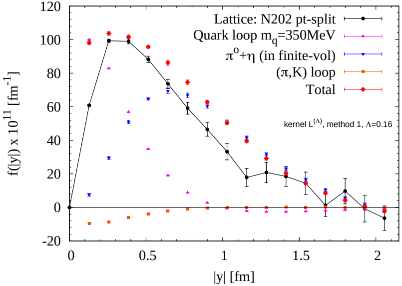

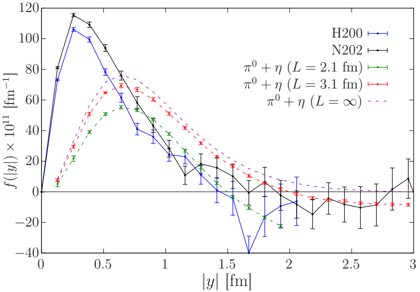

- Partial success in understanding the integrand in terms of familiar hadronic contributions.
- Reasonable understanding of magnitude of finite-size effects. ($L_{\rm H200} = 2.1\,$fm, $L_{\rm N202} = 3.1\,$fm)

2006.16224 Chao et al. (EPJC)

Separate extrapolation of conn. & disconn.

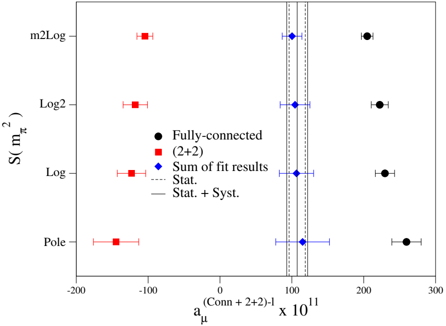

$$\text{Ansatz}: \quad Ae^{-m_\pi L/2} + Ba^2 + CS(m_\pi^2) + D + Em_\pi^2$$

- chirally singular behaviour cancels in sum of connected and disconnected.

Extrapolation to the sum of conn. & disconn.

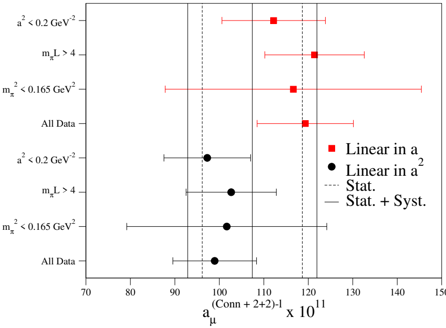

$$\text{Ansatz}: \quad Ae^{-m_\pi L/2} + Ba^2 + D + Em_\pi^2$$

- results very stable with respects to cuts in a, m_π or $m_\pi L$.
- largest systematic comes from choice of continuum limit ansatz.
- final result: central value from fitting these results with a constant; systematic error set to $\sqrt{(1/N)\sum_{i=1}^{N}(y_i - \bar{y})^2}$ as a measure of the spread of the results.

Strange contribution

Ensemble C101 ($48^3 \times 96$, $a = 0.086$ fm, $m_\pi = 220$ MeV)

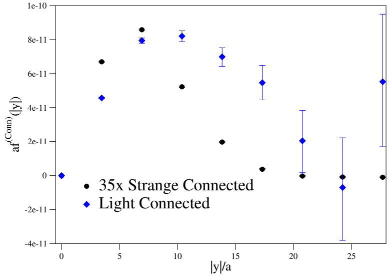

NB. Strange integrand has a factor 17 suppression due to charge factor.

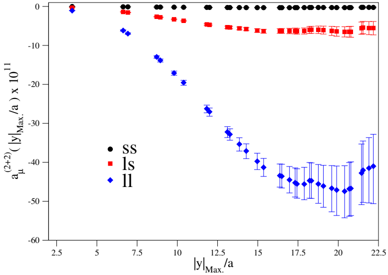

(2,2) disconnected contributions.

Extrapolation of strange contributions

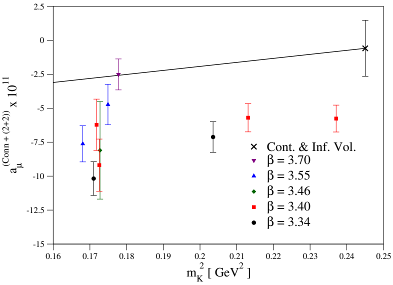

Sum of connected-strange + (2,2) topology with ss and sl quark-line content.

Final strange contribution is very small as a result of cancellations.

Compilation of a_μ^{HLbL} determinations

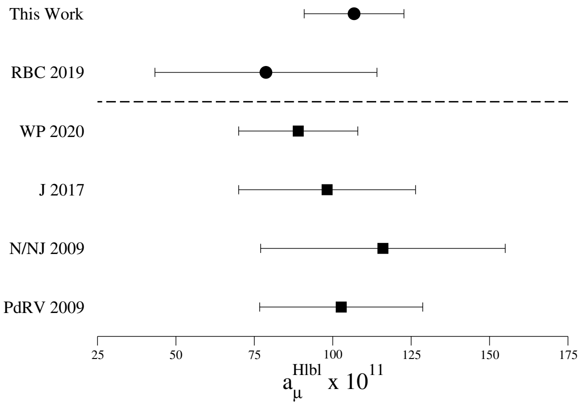

Good consistency of different determinations (not including charm here).

Fig from Chao et al, 2104.02632 (EPJC).